PHYSICAL REVIEW B VOLUME 42, NUMBER 7 1 SEPTEMBER 1990

Theory of surface spin waves in metamagnets

J. H. Baskey* and M. G. Cottam
Department of Physics, University of Western Ontario, London, Ontario, Canada N6A 3K7

(Received 24 April 1990)

A theory is presented for surface and bulk spin waves in metamagnetic materials that consist of ferromagnetically ordered layers, with the intralayer ferromagnetic exchange being much stronger than the weak antiferromagnetic coupling between adjacent layers. Results are deduced for the spin-wave dispersion relations in both the antiferromagnetic and ferromagnetic phases (depending on the applied magnetic field) at low temperatures. The results are applied to $FeBr_2$ and $FeCl_2$, where the different crystal structures lead to different properties for the surface spin waves.

I. INTRODUCTION

It is well known that at the surface of magnetic insulators there may be localized (or surface) spin waves in addition to the bulk spin waves that propagate throughout the volume of the material. There have been numerous investigations of the surface spin-wave properties of Heisenberg ferromagnets and antiferromagnets, mainly in terms of their dispersion relations, thermodynamics, and Green functions (e.g., see Refs. 1–3 for reviews).

The purpose of this paper is to extend previous studies by presenting a theory for surface spin waves in *metamagnets*. These materials have been the subject of experimental and theoretical work as regards their bulk properties for many years (e.g., see Refs. 4–7). Typically a metamagnet consists of ferromagnetically ordered layers, with the intralayer ferromagnetic exchange interactions being very much stronger than the weak antiferromagnetic interaction between adjacent layers. For small values of the magnetic field H (applied perpendicular to the layers), the adjacent layers order antiparallel to one another, giving the antiferromagnetic (AFM) phase, while for larger H (sufficient to overcome the interlayer antiferromagnetic coupling) the overall ordering is ferromagnetic (FM). The term metamagnet is usually reserved for those materials, such as $FeCl_2$ and $FeBr_2$, in which the magnetic anisotropy is sufficiently large compared with the weak antiferromagnetic coupling so that there is no spin-flop phase intermediate between the AFM and FM phases (see Ref. 5).

The spin waves in bulk samples of $FeCl_2$ and $FeBr_2$ have been studied experimentally by techniques including neutron scattering[8,9] and light scattering,[6,10,11] mainly in the AFM phase. There have also been theoretical studies of the bulk spin-wave dispersion relations and other properties (see the references above and Refs. 12 and 13) leading to satisfactory agreement with experiment.

In this work we turn our attention to surface spin waves in metamagnets. It is shown that, under certain conditions, surface spin waves are predicted to exist in semi-infinite crystals of these materials, and the dispersion relations are derived. Much of our formalism applies generally for any metamagnet, but we consider, in particular, $FeCl_2$ and $FeBr_2$. As mentioned above, these two materials have already been extensively investigated experimentally as regards their bulk spin-wave properties. Also, they differ from one another in their crystal structure, and it is shown that this leads to important differences for the surface spin-wave characteristics. In Sec. II we describe the magnetic Hamiltonian and a set of finite-difference equations satisfied by the spin-wave amplitudes is derived. These equations are solved by matrix techniques to obtain the dispersion relations of bulk and surface spin waves in both the AFM and FM phases. Specific applications to $FeBr_2$ and $FeCl_2$ are made in Sec. III, while further discussion and conclusions are given in Sec. IV.

II. SURFACE AND BULK SPIN WAVES

We write the spin Hamiltonian for a uniaxial metamagnet in the following general form (see Ref. 13):

$$\mathcal{H}=\sum_{i,j}J_{ij}(\mathbf{S}_i\cdot\mathbf{S}_j+\sigma S_i^zS_j^z)-\tfrac{1}{2}\sum_{i,i'}J'_{ii'}(\mathbf{S}_i\cdot\mathbf{S}_{i'}+\sigma' S_i^zS_{i'}^z)-\tfrac{1}{2}\sum_{j,j'}J'_{jj'}(\mathbf{S}_j\cdot\mathbf{S}_{j'}+\sigma' S_j^zS_{j'}^z)$$
$$-g\mu_B H\left[\sum_i S_i^z+\sum_j S_j^z\right]-D\left[\sum_i (S_i^z)^2+\sum_j (S_j^z)^2\right] . \quad (1)$$

Here i and i' denote sites on one sublattice (i.e., one type of layer), and j and j' denote sites on the other sublattice (the set of adjacent layers), so that J_{ij} is the interlayer antiferromagnetic exchange interaction, while $J'_{ii'}$ and $J'_{jj'}$ are the stronger intralayer ferromagnetic exchange interaction. The effect of anisotropic exchange (Ising anisotropy) can be included if parameters σ and σ' are nonzero. The applied magnetic field in the z direction (perpendicular to the layers) is denoted by H, and parameter $D>0$ characterizes the uniaxial single-ion anisotropy. We take the i sites to refer to the spin-up sublattice (with thermal average $\langle S_i^z \rangle$ positive). Hence, $\langle S_j^z \rangle$ for the other sublattice (spin down) is negative in the AFM phase, becoming positive in the FM phase for large enough value of H.

To examine the surface spin-wave excitations we consider a semi-infinite metamagnet that has a (001) surface and occupies the half-space $z \geq 0$. We label the ferromagnetically aligned layers parallel to the surface by a positive index $n(=1,2,3,\ldots)$, where $n=1$ is the surface layer, $n=2$ the next layer, and so on. We associate odd and even values of n with the spin-up and spin-down sublattices, respectively, of the AFM phase. As in previous work on semi-infinite ferromagnets and antiferromagnets (e.g., see Ref. 1), the bulk and surface spin waves can be studied by constructing the equation of motion for an S^+ operator at any site l within the semi-infinite medium, using

$$i\frac{dS_l^+}{dt}=[S_l^+,\mathcal{H}] , \tag{2}$$

where the commutator term can be evaluated in the random-phase approximation (RPA). Using translational invariance parallel to the surface, and seeking a time dependence like $\exp(-i\omega t)$ for the excitations, we write

$$S_l^+=s_n(\mathbf{k}_\parallel)\exp[i(\mathbf{k}_\parallel\cdot\boldsymbol{\rho}-\omega t)] , \tag{3}$$

where $\boldsymbol{\rho}=(x,y)$, $\mathbf{k}_\parallel=(k_x,k_y)$ is a two-dimensional wave vector, and the z coordinate of lattice point $\mathbf{r}_l$ corresponds to the layer index n. This leads to a set of linear coupled equations in the amplitudes s_n (with $n=1,2,\ldots$), and, following the procedure in Refs. 14 and 15, we may express the results equivalently in a matrix form. It is convenient at this stage to introduce two-dimensional Fourier transforms of the intralayer bulk exchange interactions by

$$u(\mathbf{k}_\parallel)=\sum_i J'_{ii'}\exp[i\mathbf{k}_\parallel\cdot(\mathbf{r}_i-\mathbf{r}_{i'})]$$
$$=\sum_j J'_{jj'}\exp[i\mathbf{k}_\parallel\cdot(\mathbf{r}_j-\mathbf{r}_{j'})] , \tag{4}$$

while for the interlayer exchange interactions we define

$$v(\mathbf{k}_\parallel)=\sum_{\boldsymbol{\delta}} J_{ij}(\boldsymbol{\delta})\exp(i\mathbf{k}_\parallel\cdot\boldsymbol{\delta}) , \tag{5}$$

where $\boldsymbol{\delta}$ is a vector joining the i sites in layer n to the j sites in layer $(n+1)$. The explicit forms of $u(\mathbf{k}_\parallel)$ and $v(\mathbf{k}_\parallel)$ depend on the crystal structure in each layer and on the stacking arrangement of the layers. Expressions appropriate to $FeBr_2$ and $FeCl_2$ will be given in Sec. III. Except where stated otherwise, we assume for simplicity that the individual exchange interactions near the surface take the same values as in the bulk.

We now present the formal results separately for the AFM and FM phases, assuming $T \ll T_c$.

A. The antiferromangetic phase

In the low-temperature limit this is the stable phase when $H<H_c$ where the bulk critical field is given approximately by

$$g\mu_B H_c=2(1+\sigma)Sv(0) . \tag{6}$$

Here S is the spin quantum number, and $\langle S_i^z \rangle = -\langle S_j^z \rangle \simeq S$ at $T \ll T_c$. The coupled equations for the spin-wave amplitudes s_n are

$$[E-g\mu_B H_A-(1+\sigma')Su(0)+Su(\mathbf{k}_\parallel)-(1+\sigma)Sv(0)]s_1-Sv(\mathbf{k}_\parallel)s_2=0 , \quad (n=1) \tag{7}$$

$$[E-g\mu_B H_A-(1+\sigma')Su(0)+Su(\mathbf{k}_\parallel)-2(1+\sigma)Sv(0)]s_{2m+1}-Sv(\mathbf{k}_\parallel)s_{2m+2}-Sv(-\mathbf{k}_\parallel)s_{2m}=0 , \quad (n=2m+1,\ \ m\geq 1) \tag{8}$$

$$[E+g\mu_B H_A+(1+\sigma')Su(0)-Su(\mathbf{k}_\parallel)+2(1+\sigma)Sv(0)]s_{2m}+Sv(\mathbf{k}_\parallel)s_{2m+1}+Sv(-\mathbf{k}_\parallel)s_{2m-1}=0 , (n=2m,\ m\geq 1) \tag{9}$$

Here we have denoted $E=\omega-g\mu_B H$, and $g\mu_B H_A=(2S-1)D$ is an effective single-ion anisotropy field. Equations (7) and (8) may be used next to eliminate the s_n terms with n odd from the set of equations represented by (9). The resulting equations connecting the s_n with n even can be written in a matrix form as

$$(A_0+\Delta)F=0 , \tag{10}$$

where F is an infinite-dimensional column matrix whose elements are specified by $F_m=s_{2m}$ and A_0 is a tridiagonal matrix:

$$A_0=\begin{bmatrix} d & -\tau^{-1} & 0 & .. & & & \\ -\tau & d & -\tau^{-1} & 0 & \cdots & & \\ 0 & -\tau & d & -\tau^{-1} & 0 & \cdots & \\ 0 & 0 & -\tau & d & -\tau^{-1} & 0 & \cdots \\ \vdots & \vdots & \vdots & \vdots & \vdots & \vdots & \end{bmatrix} \tag{11}$$

with

$$d=\frac{\{[g\mu_B H_A+(1+\sigma')Su(0)-Su(\mathbf{k}_\parallel)+2(1+\sigma)Sv(0)]^2-E^2\}}{S^2v(\mathbf{k}_\parallel)v(-\mathbf{k}_\parallel)}-2\ , \tag{12}$$

$$\tau=v(-\mathbf{k}_\parallel)/v(\mathbf{k}_\parallel)\ . \tag{13}$$

The matrix Δ in (10) describes the perturbing effect of the surface, and in the present case it is given simply by

$$\Delta_{m,m'}=\Delta_0\delta_{m,1}\delta_{m',1}$$

with

$$\Delta_0=(1+\sigma)Sv(0)/[E-g\mu_B H_A-(1+\sigma')Su(0)+Su(\mathbf{k}_\parallel)-(1+\sigma)Sv(0)]\ . \tag{14}$$

We now write $(A_0+\Delta)=A_0(I+B\Delta)$, where I is the unit matrix and $B=A_0^{-1}$. Following the matrix formalism as used in Refs. 14 and 15 for other surface problems, the surface spin-wave solutions correspond to

$$\det(I+B\Delta)=0\ . \tag{15}$$

This is easily evaluated using the result that the inverse of A_0 is known exactly (generalizing Refs. 14 and 15) as

$$B_{m,m'}=\begin{cases}\tau(\tau^{2m}x^{m+m'}-x^{m'-m})/(\tau^2x-x^{-1}), & m\le m'\\ \tau^{2m+1}(x^{m+m'}-\tau^{-2m'}x^{m-m'}/(\tau^2x-x^{-1})\ , & m>m'\end{cases} \tag{16}$$

where x is a complex quantity satisfying $|x|\le 1$ and

$$\tau x+(\tau x)^{-1}=d\ . \tag{17}$$

On substituting Eqs. (14) and (16) into (15) and simplifying, we obtain the conditions for a surface spin wave to be

$$x=-1/(\tau\Delta_0)\ . \tag{18}$$

When this is substituted into (17) we obtain an expression that can be solved for the energy E corresponding to the surface spin waves. The x parameter is related to the attenuation of a surface spin wave through the property $|x|=\exp(-2\lambda c_0)$, where $2c_0$ represents the distance between adjacent even-index layers (i.e., c_0 is the layer separation) and $\lambda>0$ is an attenuation factor (see Ref. 15). Hence, we have $|x|<1$ as a necessary condition for the existence of a surface spin-wave branch.

By contrast, the bulk spin waves correspond to $|x|=1$ (cf., Ref. 15). On putting $x=\exp(2ik_zc_0)$ in (17), where k_z is the third component of the three-dimensional wave vector $\mathbf{k}=(\mathbf{k}_\parallel,k_z)$, and solving for E, we obtain the dispersion relation

$$\begin{aligned}E^2=[g\mu_B H_A+(1+\sigma')Su(0)-Su(\mathbf{k}_\parallel)+2(1+\sigma)Sv(0)]^2\\ -S^2v(\mathbf{k}_\parallel)v(-\mathbf{k}_\parallel)[2+\tau\exp(2ik_zc_0)\\ +\tau^{-1}\exp(-2ik_zc_0)]\ .\end{aligned} \tag{19}$$

B. The ferromagnetic phase

The spin-wave analysis is more straightforward in this case (which applies for $H>H_c$) because the direction of net spin alignment is the same on both sublattices and there is no need to treat the layers with n even and n odd differently. The coupled equations for the spin-wave amplitudes s_n at $T\ll T_c$ (where now $\langle S_i^z\rangle=\langle S_j^z\rangle\simeq S$) become

$$[E-g\mu_B H_A-(1+\sigma')Su(0)+Su(\mathbf{k}_\parallel)+(1+\sigma)Sv(0)]s_1-Sv(\mathbf{k}_\parallel)s_2=0,\quad (n=1)\ . \tag{20}$$

$$[E-g\mu_B H_A-(1+\sigma')Su(0)+Su(\mathbf{k}_\parallel)+2(1+\sigma)Sv(0)]s_n-Sv(\mathbf{k}_\parallel)s_{n+1}-Sv(-\mathbf{k}_\parallel)s_{n-1}=0,\quad (n\ge 2)\ , \tag{21}$$

where we employ the same notation as in the preceding subsection. They can be written directly in the same matrix form as Eqs. (10)–(14) with the following redefinitions. The general element of matrix F is now specified by $F_n=s_n$ and we have

$$d=-[g\mu_B H_A+(1+\sigma')Su(0)-Su(\mathbf{k}_\parallel)-2(1+\sigma)Sv(0)-E]/S|v(\mathbf{k}_\parallel)|\ , \tag{22}$$

$$\tau=v(-\mathbf{k}_\parallel)/|v(\mathbf{k}_\parallel)|\ , \tag{23}$$

$$\Delta_0=-(1+\sigma)v(0)/|v(\mathbf{k}_\parallel)|\ . \tag{24}$$

The same formalism as for the AFM phase can now be followed. In particular, the x value corresponding to a surface spin wave is again given formally by (18) provided the existence (localization) condition that $|x|<1$ is satisfied. The surface spin-wave dispersion relation is obtained from (17), (18), and (22)–(24).

The bulk spin-wave dispersion relation is obtained by substituting $x=\exp(ik_z c_0)$ into (17) and using (22) and (23):

$$E=g\mu_B H_A+(1+\sigma')Su(0)-Su(\mathbf{k}_\parallel)-2(1+\sigma)Sv(0)$$
$$+S|v(\mathbf{k}_\parallel)|[\tau\exp(ik_z c_0)+\tau^{-1}\exp(-ik_z c_0)] \ . \qquad (25)$$

III. APPLICATION TO $\mathrm{FeBr_2}$ AND $\mathrm{FeCl_2}$

We now discuss the results of the preceding section in more detail for the specific cases of $\mathrm{FeBr_2}$ and $\mathrm{FeCl_2}$. These metamagnets have different crystallographic arrangements of the magnetic ions, leading to differences in the spin-wave spectra.

Both materials have the same trigonal arrangement of magnetic $\mathrm{Fe^{2+}}$ ions within each ferromagnetically ordered layer (see Fig. 1). We denote by J_1 and J_2 the dominant nearest-neighbor exchange and the weaker next-nearest-neighbor exchange, respectively. Hence, the intralayer exchange sum $u(\mathbf{k}_\parallel)$ defined in Eq. (4) is given by

$$u(\mathbf{k}_\parallel)=2J_1[\cos(k_x a)+2\cos(k_x a/2)\cos(k_y a\sqrt{3}/2)]$$
$$+2J_2[\cos(k_y a\sqrt{3})$$
$$+2\cos(k_y a\sqrt{3}/2)\cos(k_x a3/2)] \ , \qquad (26)$$

where a is the nearest-neighbor distance in the layers and the choice of coordinate axes is indicated in Fig. 1.

The two materials differ, however, in the stacking arrangement of the layers. In $\mathrm{FeBr_2}$ the $\mathrm{Fe^{2+}}$ ions in one layer are directly above and below those in the adjacent layers. The very weak antiferromagnetic exchange interaction, denoted by J_3, couples to the one nearest neighbor in each adjacent layer and we have, for the interlayer exchange sum defined in Eq. (5),

$$v(\mathbf{k}_\parallel)=J_3 \quad (\text{for FeBr}_2) \ . \qquad (27)$$

By contrast, the stacking of the layers is staggered in the case of $\mathrm{FeCl_2}$ (see Fig. 1). There are three nearest neighbors in each of the adjacent layers and we have

$$v(\mathbf{k}_\parallel)=J_3[\exp(ik_y a/\sqrt{3})$$
$$+2\cos(k_x a/2)\exp(-ik_y a/2\sqrt{3})]$$
$$(\text{for FeCl}_2) \ . \qquad (28)$$

The distance c_0 between layers is equal to c and $c/3$ for $\mathrm{FeBr_2}$ and $\mathrm{FeCl_2}$, respectively, where c denotes the distance along the c axis of the conventional magnetic unit cell for each case.

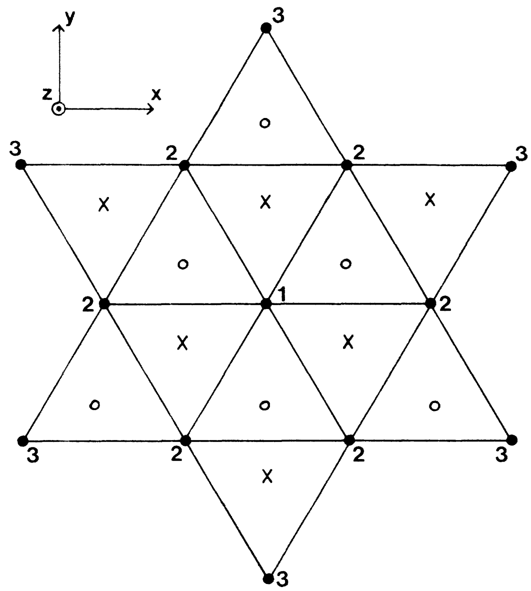

FIG. 1. Planar view of the triangular arrangement of $\mathrm{Fe^{2+}}$ ions (solid circles) in the ferromagnetically ordered layers for $\mathrm{FeBr_2}$ and $\mathrm{FeCl_2}$. The nearest- and next-nearest intralayer neighbors to the ion labeled 1 are those labeled 2 and 3, respectively. In $\mathrm{FeBr_2}$ the ions in adjacent layers are vertically above and below the solid circles. In $\mathrm{FeCl_2}$ the layers are staggered with respect to one another, and the crosses and open circles represent the positions of the ions in the adjacent layers above and below the plane.

A. Results for $\mathrm{FeBr_2}$

This material has spin $S=1$ and critical temperature $T_c=14.2$ K. The lattice constants are $a=3.75$Å and $c=12.38$Å (see Ref. 16). The approximate values of the exchange and anisotropy parameters are known from neutron-scattering and Raman-scattering experiments,[9,11] and here we take $J_1=5.07\ \mathrm{cm^{-1}}$, $J_2=-1.2\ \mathrm{cm^{-1}}$, $J_3=1.45\ \mathrm{cm^{-1}}$, $D=7.34\ \mathrm{cm^{-1}}$, and $\sigma=\sigma'=0.28$.

In the AFM phase the formal expression (19) for the bulk spin-wave frequency simplifies because $v(\mathbf{k}_\parallel)$ is real and independent of $\mathbf{k}_\parallel$ for $\mathrm{FeBr_2}$. The result for the two branches becomes $\omega=\omega_B^\pm(\mathbf{k})$, where

$$\omega_B^\pm(\mathbf{k})=g\mu_B H\pm\{[E_0(\mathbf{k}_\parallel)+2(1+\sigma)SJ_3]^2$$
$$-[2SJ_3\cos(k_z c)]^2\}^{1/2} \ . \qquad (29)$$

Here $E_0(\mathbf{k}_\parallel)$ is defined by

$$E_0(\mathbf{k}_\parallel)=g\mu_B H_A+(1+\sigma')Su(0)-Su(\mathbf{k}_\parallel) \ , \qquad (30)$$

and Eqs. (29) and (30) are in agreement, as expected, with previous spin-wave theories for an *infinite* $\mathrm{FeBr_2}$ crystal.[11] From (12), (14), (17), and (18), it follows that there are surface spin-wave solutions given by $\omega=\omega_S^\pm(\mathbf{k}_\parallel)$ where

$$\omega_S^{\pm}(\mathbf{k}_{\parallel})=g\mu_B H - A \pm \{[E_0(\mathbf{k}_{\parallel})+(1+\sigma)SJ_3 + A]^2 - (SJ_3)^2\}^{1/2} \tag{31}$$

with

$$A=\sigma(2+\sigma)SJ_3/[2(1+\sigma)] \ . \tag{32}$$

The above surface spin-wave branches only exist provided the localization condition $|x|<1$ (see Sec. II) is satisfied, and in the present case give the requirement for a physical solution that

$$|E_0(\mathbf{k}_{\parallel})+(1+\sigma)SJ_3-\omega_S^{\pm}(\mathbf{k}_{\parallel})+g\mu_B H| < (1+\sigma)SJ_3 \ . \tag{33}$$

For most values of the parameters (including those appropriate to FeBr$_2$) the above condition implies that only the $\omega_S^{+}(\mathbf{k}_{\parallel})$ is physical. Numerical calculations of the predicted bulk and surface spin-wave dispersion relations for FeBr$_2$ in zero applied field ($H=0$) are shown in Figs. 2 and 3 for the cases of the parallel wave vector $\mathbf{k}_{\parallel}$ along the x and y directions, respectively. We have shown only the positive-frequency solutions, because the two branches to the bulk spin-wave spectrum in the AFM phase are degenerate in magnitude ($|\omega_B^{+}|=|\omega_B^{-}|$) when $H=0$. The bulk modes are specified by a three-dimensional wave vector $\mathbf{k}=(\mathbf{k}_{\parallel},k_z)$, and so should appear as a band in such a plot because of the range of possible values for k_z. However, in the present case, J_3 is relatively small and the dispersion relation (29) is a quadratic expression, with the consequence that the dependence on k_z is almost negligible in the AFM phase. It is seen from Figs. 2 and 3 that the surface spin-wave branch is split off below the bulk modes by about 2 cm^{-1}. This separation is sufficiently large to be resolved using Raman scattering.

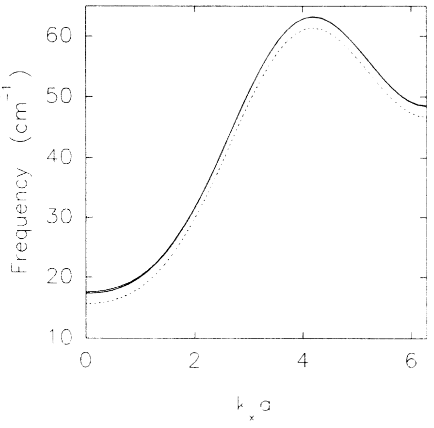

FIG. 2. Dispersion relations of bulk and surface spin waves in FeBr$_2$ in the AFM phase, taking $H=0$ for the applied field and the parallel wave vector $\mathbf{k}_{\parallel}$ along the x direction. The bulk spin-wave frequencies (solid lines) form a band because of the range of k_z values, but this k_z dependence is very small in the present case. The surface spin-wave branch is shown by a dashed line.

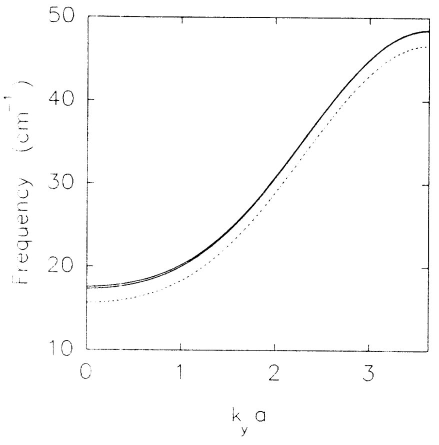

FIG. 3. The same as for Fig. 2 for FeBr$_2$ in the AFM phase, but with $\mathbf{k}_{\parallel}$ along the y direction.

In the FM phase, the corresponding results for the bulk spin-wave frequency $\omega_B(\mathbf{k})$ and the surface spin-wave frequency $\omega_S(\mathbf{k}_{\parallel})$ become

$$\omega_B(\mathbf{k})=g\mu_B H+E_0(\mathbf{k}_{\parallel})-2(1+\sigma)SJ_3 +2SJ_3\cos(k_z c) \ , \tag{34}$$

$$\omega_S(\mathbf{k}_{\parallel})=g\mu_B H+E_0(\mathbf{k}_{\parallel})-(1+\sigma)SJ_3 +(1+\sigma)^{-1}SJ_3 \ . \tag{35}$$

The existence (localization) condition for the surface spin-wave branch is simply $\sigma>0$. This is satisfied for FeBr$_2$, and numerical estimates show that $\omega_S(\mathbf{k}_{\parallel})>\omega_B(\mathbf{k})$ with $\mathbf{k}=(\mathbf{k}_{\parallel},k_z)$ and for any value of k_z in the Brillouin zone. However, the splitting of the surface spin wave above the bulk modes is too small (about 0.1 cm^{-1}) in FeBr$_2$ to be observed by conventional Raman scattering.

B. Results for FeCl$_2$

The lattice constants of FeCl$_2$ ($S=1$ and $T_c=23.5$ K) are given by $a=3.58$Å and $c=17.54$Å (see Ref. 16). For the exchange and anisotropy parameters we take $J_1=5.5$ cm^{-1}, $J_2=-1.2$ cm^{-1}, $J_3=0.28$ cm^{-1}, $D=9.4$ cm^{-1}, and $\sigma=\sigma'=0.2$, in accordance with data from neutron and Raman scattering.[10,13,17]

For the FeCl$_2$ structure the interlayer term $v(\mathbf{k}_{\parallel})$ is a complex function of $\mathbf{k}_{\parallel}$ [see Eq. (28)], and this makes some of the results more complicated than in the FeBr$_2$

case. In the AFM phase we find the following expressions for the bulk and surface spin-wave frequencies:

$$\omega_B^{\pm}(\mathbf{k})=g\mu_B H\pm\{[E_0(\mathbf{k}_\parallel)+6(1+\sigma)SJ_3]^2-[2SJ_3\alpha_B(\mathbf{k})]^2\}^{1/2}\,, \tag{36}$$

$$\omega_S^{\pm}(\mathbf{k}_\parallel)=g\mu_B H-A'\pm\{[E_0(\mathbf{k}_\parallel)+3(1+\sigma)SJ_3+A']^2-[SJ_3\alpha_S(\mathbf{k}_\parallel)]^2\}^{1/2}\,. \tag{37}$$

Here $E_0(\mathbf{k}_\parallel)$ is defined in Eq. (30), and

$$A'=\left[\frac{3}{2}(1+\sigma)-\frac{1}{6(1+\sigma)}\alpha_S^2(\mathbf{k}_\parallel)\right]SJ_3\,, \tag{38}$$

while $\alpha_B(\mathbf{k})$ and $\alpha_S(\mathbf{k}_\parallel)$ denote

$$\mathrm{Re}[\exp(-ik_z c/3)v(\mathbf{k}_\parallel)]/J_3$$

and $|v(\mathbf{k}_\parallel)|/J_3$, respectively, or explicitly,

$$\alpha_B(\mathbf{k})=\cos(k_y a/\sqrt{3}-k_z c/3)+\cos(k_y a/2\sqrt{3}+k_x a/2+k_z c/3)+\cos(k_y a/2\sqrt{3}-k_x a/2+k_z c/3)\,, \tag{39}$$

$$\alpha_S(\mathbf{k}_\parallel)=|4\cos^2(k_x a/2)+4\cos(k_x a/2)\cos(k_y a\sqrt{3}/2)+1|^{1/2}\,. \tag{40}$$

In this case the existence condition for either of the surface branches $\omega_S^{\pm}(\mathbf{k}_\parallel)$ to represent a physical solution is

$$|E_0(\mathbf{k}_\parallel)+3(1+\sigma)SJ_3-\omega_S^{\pm}(\mathbf{k}_\parallel)+g\mu_B H|<3(1+\sigma)SJ_3\,, \tag{41}$$

and for most values of the parameters (including those taken for FeCl$_2$) this will be satisfied only by $\omega_S^{+}(\mathbf{k}_\parallel)$. Numerical calculations to illustrate the predicted bulk and surface spin-wave dispersion relations for FeCl$_2$ are shown in Figs. 4 and 5 for two different directions of $\mathbf{k}_\parallel$.

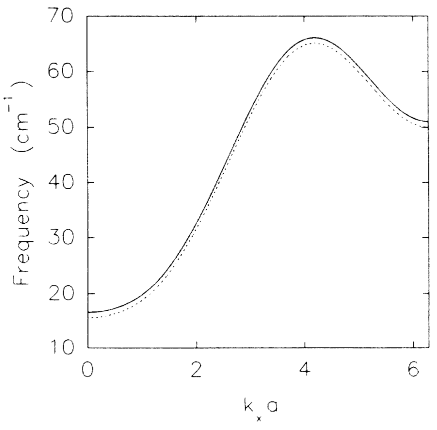

FIG. 4. Dispersion relations of bulk spin waves (solid lines) and surface spin waves (dashed line) in FeCl$_2$ in the AFM phase, taking $H=0$ for the applied field and the parallel wave vector $\mathbf{k}_\parallel$ along the x direction.

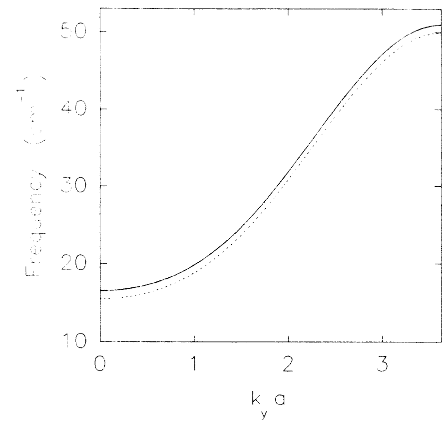

FIG. 5. The same as for Fig. 4 for FeCl$_2$ in the AFM phase, but with $\mathbf{k}_\parallel$ along the y direction.

The qualitative behavior is similar to that for FeBr$_2$, but the surface branch is split off by only about 1 cm^{-1} because J_3 is smaller than for FeBr$_2$ and the crystal structure is different.

In the FM phase of the FeCl$_2$ structure, the results for the bulk and surface spin-wave frequencies are

$$\omega_B(\mathbf{k})=g\mu_B H+E_0(\mathbf{k}_\parallel)-6(1+\sigma)SJ_3+2SJ_3\alpha_B(\mathbf{k})\,, \tag{42}$$

$$\omega_S(\mathbf{k}_\parallel)=g\mu_B H+E_0(\mathbf{k}_\parallel)-3(1+\sigma)SJ_3+\tfrac{1}{3}(1+\sigma)^{-1}SJ_3\alpha_S^2(\mathbf{k}_\parallel)\,. \tag{43}$$

In this case the surface spin-wave branch exists provided $\sigma>-\frac{2}{3}$, which is satisfied for FeCl$_2$. A numerical example is given in Fig. 6, where it can be seen that the surface spin-wave branch comes above the bulk band. The splitting is negligible for small $|\mathbf{k}_\parallel|$ but (unlike the case of FeBr$_2$) it becomes larger and of order 1 cm^{-1} for larger

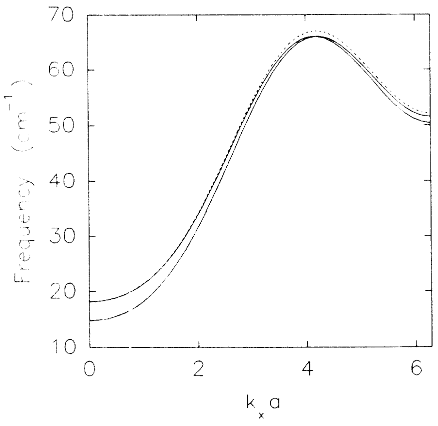

FIG. 6. Dispersion relations of bulk and surface spin waves in FeCl$_2$ in the FM phase, taking $g\mu_B H=4$ cm^{-1} for the applied field and the parallel wave vector $\mathbf{k}_\parallel$ along the x direction. In this case the broadening of the bulk spin waves into a band (region between the solid lines) is apparent, and the surface spin-wave branch is shown by a dashed line.

wave vectors as a consequence of the different crystal structure.

IV. CONCLUSIONS

In this paper we have presented a theory for the surface (and bulk) spin waves in semi-infinite metamagnets at low temperatures $T \ll T_c$ and in both the AFM and FM phases. In these materials there are competing ferromagnetic and antiferromagnetic exchange terms, as well as a large single-ion anisotropy, and our method of calculation is an extension of previous theoretical work for ferromagnets and antiferromagnets. The theoretical results were applied to the metamagnets $FeBr_2$ and $FeCl_2$, which have a different crystal structure leading to a difference in the surface spin-wave dispersion relations and existence conditions. The spin-wave properties in bulk samples of both of these materials have already been extensively studied by Raman scattering and other experimental techniques, as mentioned in Sec. I. It would be of interest to have similar experiments carried out to study the surface spin waves. This might be done, for example, by Raman techniques using a backscattering geometry to scatter light from a single surface of a metamagnet, by analogy with other surface light-scattering studies (see Ref. 6). The theoretical results in this paper indicate that the surface spin waves are separated in frequency from the bulk spin waves to a larger extent in the AFM phase and this would make the surface spin waves more readily observable by Raman scattering. Also, we calculated a larger frequency separation in $FeBr_2$ compared with $FeCl_2$, which would favor the former material for experimental studies.

On the theoretical side, there are various possible extensions to this work. These include incorporating the effects of modified exchange constants at the surface and carrying out Green-function calculations. The former would lead to a modification of the frequency separation between bulk and surface spin waves (which is expected to be more important in the FM phase), whereas the latter would be needed for calculating Raman-scattering intensities.

ACKNOWLEDGMENTS

This work was supported in part by the Natural Sciences and Engineering Research Council of Canada (NSERC).

---

*Present address: Department of Applied Physics, Harvard University, Cambridge, MA 02138.

[1] T. Wolfram and R. E. DeWames, Prog. Surf. Sci. **2**, 233 (1972).

[2] M. G. Cottam and A. A. Maradudin, in *Surface Excitations*, edited by V. M. Agranovich and R. Loudon (North-Holland, Amsterdam, 1984), p. 1.

[3] D. L. Mills, in *Surface Excitations*, edited by V. M. Agranovich and R. Loudon (North-Holland, Amsterdam, 1984), p. 379.

[4] I. S. Jacobs and P. E. Lawrence, Phys. Rev. **164**, 866 (1967).

[5] L. J. De Jongh and A. R. Miedema, *Experiments on Simple Magnetic Model Systems* (Taylor and Francis, London, 1974), p. 88.

[6] M. G. Cottam and D. J. Lockwood, *Light Scattering in Magnetic Solids* (Wiley, New York, 1986), p. 118.

[7] J. F. Dillon, Jr., E. Yi Chen, and H. J. Guggenheim, Phys. Rev. B **15**, 1422 (1977).

[8] C. Vettier and W. B. Yelon, Phys. Rev. B **11**, 4700 (1975).

[9] W. B. Yelon and C. Vettier, J. Phys. C **8**, 2760 (1975).

[10] D. J. Lockwood, G. Mischler, A. Zwick, I. W. Johnstone, G. C. Psaltakis, M. G. Cottam, S. Legrand, and J. Leotin, J. Phys. C **15**, 2793 (1982).

[11] G. C. Psaltakis, G. Mischler, D. J. Lockwood, M. G. Cottam, A. Zwick, and S. Legrand, J. Phys. C **17**, 1735 (1984).

[12] M. G. Pini, E. Rastelli, A. Tassi, and V. Tognetti, J. Phys. C **14**, 3041 (1981).

[13] G. C. Psaltakis and M. G. Cottam, J. Phys. C **15**, 4847 (1982).

[14] R. E. DeWames and T. Wolfram, Phys. Rev. **185**, 720 (1969).

[15] M. G. Cottam, J. Phys. C **9**, 2121 (1976).

[16] R. W. Wyckoff, *Crystal Structures* (Interscience, New York, 1963), Vol. 1, p. 266.

[17] W. B. Yelon and R. J. Birgeneau, Phys. Rev. B **5**, 2615 (1972).